Focus on the mechatronics design of a new dexterous robotic hand for inside hand manipulation

P. Vulliez, J. P. Gazeau*, P. Laguillaumie,
H. Mnyusiwalla, P. Seguin

Mechanical Engineering and Complex Systems Department, PPRIME Institute, CNRS - University of Poitiers - ENSMA - UPR 3346, Chasseneuil Futuroscope 86962, France

SUMMARY

This paper presents a novel tendon-driven bio-inspired robotic hand design for in-hand manipulation. Many dexterous robot hands are able to produce adaptive grasping, but only a few human-sized hands worldwide are able to produce fine motions of the object in the hand. One of the challenges for the near future is to develop human-sized robot hands with human dexterity. Most of the existing hands considered in the literature suffer from dry friction which creates unwanted backlash and non-linearities. These problems limit the accurate control of the fingers and the capabilities of the hand. Such was the case with our first fully actuated dexterous robot hand: the Laboratoire de Mécanique des Solides (LMS) hand.

The mechanical design of the hand relies on a tendon-based transmission system. Developing a fully actuated dexterous robot hand requires the routing of the tendons through the finger for the actuation of each joint. This paper focuses on the evolution of the tendon routing; from the LMS hand to the new RoBioSS dexterous hand. The motion transmission in the new design creates purely linear coupling relations between joints and actuators. Experimental results using the same protocol for the previous hand and the new hand illustrate the evolution in the quality of the mechanical design. With the improvements of the mechanical behavior of the robotic fingers, the hand control software could be extensively simplified. The choice of a common architecture for all fingers makes it possible to consider the hand as a collaboration of four serial robots. Moreover, with the transparency of the motor-joint transmissions, we could use robust, industrial-grade cascaded feedback loops for the axis controls.

An inside-hand manipulation task concerning the manipulation of a bottle cap is presented at the end of the paper. As proof of the robustness of the hand, demonstrations of the hand's capabilities were carried out continuously over three days at SPS IPC Drives international exhibition in Nuremberg, in November 2016.

KEYWORDS: Mechanical hand, Gripper, Dexterous manipulation, Finger design, Dexterous hand, Tendon routing, Mechatronic design

1. From the LMS Hand to a New Hand Specification

1.1. Introduction

To bring robots into the home or other unstructured environments, one key requisite is a universal end-effector, which will enable the robot to interact with other *in-situ* actors. One of the best existing designs in nature for this kind of interface is, of course, the human hand, and for many years researchers have been trying to mimic it. As a consequence, several successful designs of anthropomorphic hands have been presented in the literature.[1−5] There is, however, still room for improvement to reach the levels of performance of a human hand, especially in terms of dexterity.

As an illustration of these challenges, a roadmap for human-like dexterous manipulation is specified by the US National Institute of Standards and Technology.[6] In the next 5 years, low complexity hands,

* Corresponding author. E-mail: jean.pierre.gazeau@univ-poitiers.fr

with small numbers of independent joints are expected to be capable of robust whole-hand grasping. Furthermore, in the next 15 years, high-complexity hands with a tactile sensing approaching the ones of humans should be capable of robust whole-hand grasp and dexterous manipulation of objects present in manufacturing environment and used by human workers.

That being said, it is still difficult to meet all these requirements in a single device. None of the existing hands can fulfill these requirements. As an example, many famous robot hands are capable of adaptive grasping, but producing fine motions of objects within the hand remains a complex problem as discussed in ref. [7]. The challenge is that each finger needs to collaborate in a synchronous way with the other fingers involved in the grasp, in order to produce the desired object motion.

In the videos available of the famous "Shadow" robot hand,[8,9] fine and accurate manipulation of an object inside the hand, involving synchronized movement of fingers, is not demonstrated; either the hand grasps the objects, or the fingers can be moved freely by using a dataglove. This is also the case for the NASA hand.[10] This hand is able to grasp objects but not to produce a fine motion of the object held in the hand. For the Commissariat à l'Energie Atomique (CEA) dexterous robot hand,[11] it is still difficult to show an effective synchronization of the fingers and at the same time an accurate motion of the grasped object inside the hand. The Metahand Robot Hand that features three fingers and an articulated palm[12] does not demonstrate smooth and continuous movements of the object grasped in the hand with a high level of synchronization. The high speed hand from Tokyo University, which requires a high speed vision tracking system,[13] is able to produce inside hand manipulation with high dynamics, as illustrated with the pen spinning task. But this example does not demonstrate the capability of the hand for producing any fine motions of the object inside the hand; no video is available that illustrates such fine motions.

Robotic hands are often driven by cables.[2,13,15,16,17,25] Several approaches have been proposed for tendon-driven finger design. To lower the complexity of the problem, some underactuated robotic hands have been developed in academic labs[18,19] and prosthetic devices like the Spring Hand[20] or artificial muscle actuated finger[14] and commercial prosthetic hands: the i-Limb hand or the Ottobock Michelangelo hand are available. In these devices, a reduced number of actuators are employed, and the non-actuated degrees of freedom (DoF) are coupled with others. Most of these devices allow the execution of stable grasps but do not propose in-hand manipulation capabilities.

Our work focuses on the development of a novel modular finger design for the purpose of providing a highly dexterous hand. One way to increase the dexterity of a robotic hand is to improve its capacity for in-hand manipulation, which can be achieved by a better controllability of the fingers. The main impediment for good control of tendon-driven robotic fingers is friction, which, incidentally, leads to rapid cable wear. That was the case with our first hand[21] as will be detailed in this paper. Other hands also suffer from this issue, for example, the joint position controller of the Shadow Hand lacks accuracy, which leads to unrepeatable finger movements.[8]

Based on our experience with the development of LMS hand,[1,21] we are now able to propose a novel anthropomorphic finger design, which minimizes friction and improves the controllability of all joints (CNRS Patent).[22] The bio-inspired finger design was presented in a previous paper.[23] This present paper focuses on the evolution of the mechatronics design proposed with the RoBioSS hand for inside hand manipulation purposes. One of the challenges, compared to the previous hand, was to make the synchronization of the fingers possible by maximizing the transparency of transmission.

This paper is organized as follows. Before presenting the evolution in the new hand design, we show the background of our design choices by detailing the issues encountered by our first hand. Section 2 presents the kinematics of the new hand. The tendon routing is detailed, and the design choices for the metacarpophalangeal joint (MCP) are explained in Section 3. Section 4 details the experimental study that validates the finger design. The last section summarizes the work and explores potential future research.

1.2. Analysis of the LMS HAND limitations
The LMS hand shown in Fig. 1 was the first dexterous hand of the RoBioSS team designed for inside hand manipulation. The motion transmissions between the actuators located in the forearm and the joints are based on the use of polyethylene cables. It has 16 fully actuated DoF, and 4 joints for each finger. The LMS hand is also discussed and compared to other hands in ref. [24].

In tendon-based actuation, one fundamental design issue is how tendons are routed from motors to joints. For the LMS hand, the choice of sheaths and guiding pulleys was made to keep the cable length
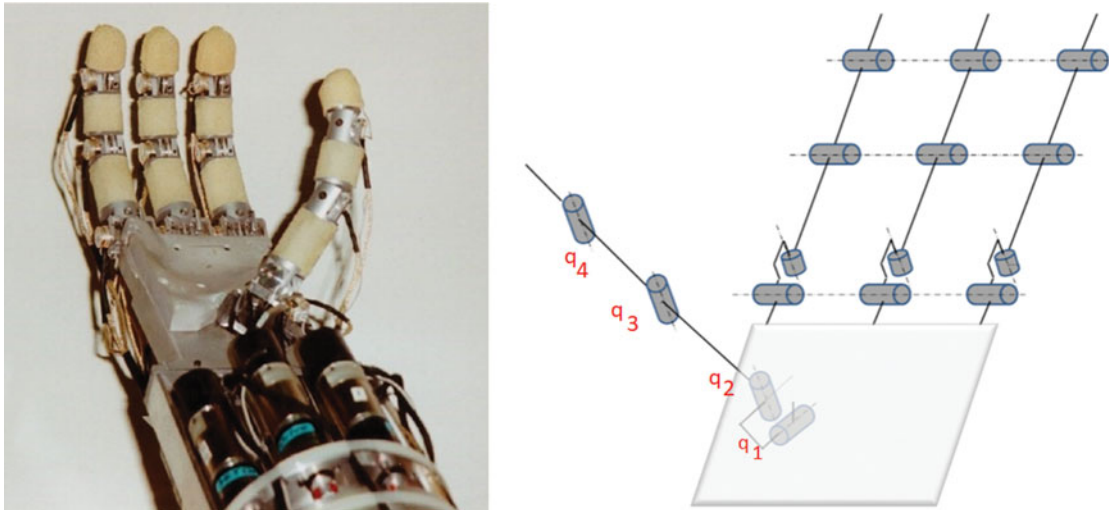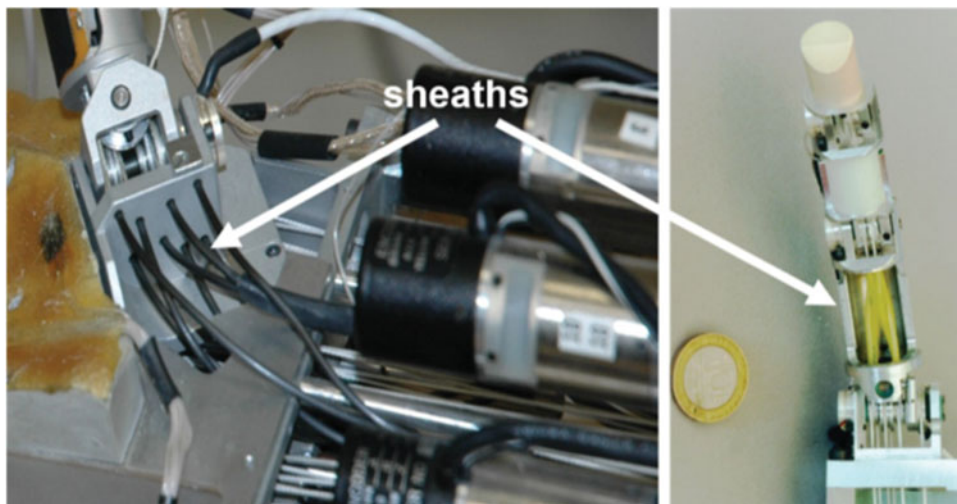
Fig. 1. The LMS hand.

Fig. 2. A transmission based on the use of sheathed cables, thumb (left) and one of the fingers (right).

constant between each actuator and the corresponding joint. The first disadvantage of this solution is that the use of guiding surfaces on which the cable slides naturally involves friction. Figure 2 presents the routing of the tendons and the sheaths involved in the motion transmission for the LMS hand at the MCP joint. The second disadvantage concerns the fact that the small sheaths deform because of the residual cable tension.

All the pulleys in the transmission have the same diameters; thus, theoretical coupling relations between the motor positions and the joints are as follows:

$$Q = A_{\text{thumb}} \cdot S$$

$$A_{\text{thumb}} = \begin{bmatrix} 1 & 0 & 0 & 0 \\ 0 & 1 & 0 & 0 \\ 0 & 0 & 1 & 0 \\ 0 & 0 & 1 & 1 \end{bmatrix}$$

where

$Q = [q_1 q_2 q_3 q_4]^T$ represents the thumb joints values as presented in Fig. 1
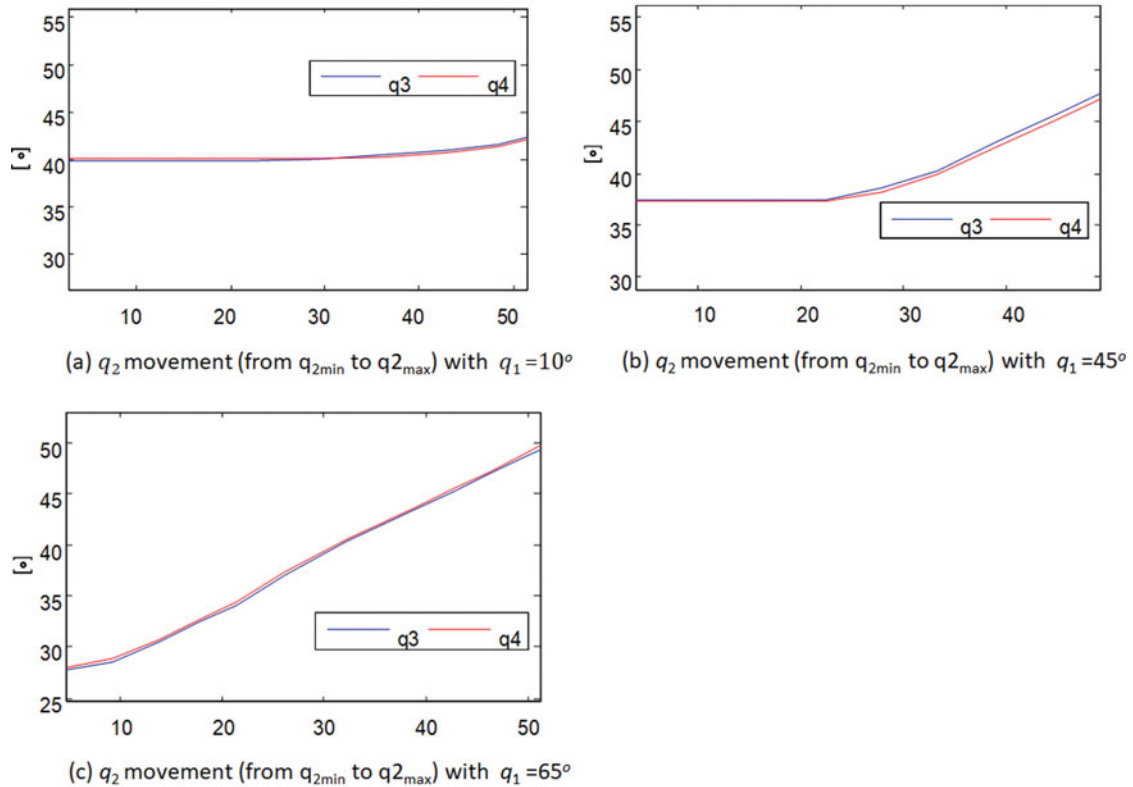$S = [s_1 s_2 s_3 s_4]^T$ represents the actuator positions.

(a) q_2 movement (from q_{2min} to q_{2max}) with $q_1 = 10°$

(b) q_2 movement (from q_{2min} to q_{2max}) with $q_1 = 45°$

(c) q_2 movement (from q_{2min} to q_{2max}) with $q_1 = 65°$

Fig. 3. Measures of q3 and q4 while moving q2 for different fixed values of q1.

Figure 3 illustrates the experimental evaluation of the LMS hand. We can clearly see that a non-desired coupling relation exists between the joints: when q_2 moves q_3 and q_4 start moving at different positions and in different ways depending on the value of q_1.

To take into account this non-linear coupling, we adapted the coupling matrix A_{thumb} in the following way in order to reproduce the real motion relations due to the behavior of the transmission:

$$A_{\text{thumb}} = \begin{bmatrix} 1 & 0 & 0 & 0 \\ 0 & 1 & 0 & 0 \\ 0 & & 1 & 0 \\ 0 & & 1 & 1 \end{bmatrix}$$

To determine the coefficient α which integrates the non-linearity of the transmission, we used fuzzy logic. This method allows the estimation of the variable coupling coefficient with a minimum amount of data; Fig. 4 shows the values of α. This coefficient takes into account the coupling between the joints q3 and q4 and the two other joints q1 and q2. More details on the implementation of the fuzzy controller can be found in ref. [1]

The fuzzy logic controller enabled us to control the hand for grasping various objects as shown in Fig. 5. However, it was not able to perform inside hand manipulation with the fingertips, as this kind of task required the ability to control each finger in a coordinated way. We concluded that the behavior of each finger had to be precise, reproducible and identical. We therefore focused on these constraints for the new finger design, and, as a result of this, we decided to avoid the use of sheaths for tendon routing.

2. New Hand Kinematics

Based on this experience and on the work on the ANR ABILIS project (http://abilis.lms.sp2mi.univ-poitiers.fr/), we decided in 2013 to propose a more efficient design, able to meet challenges from the US National Institute roadmap.[6] Our new goals were to create a human-sized anthropomorphic hand,
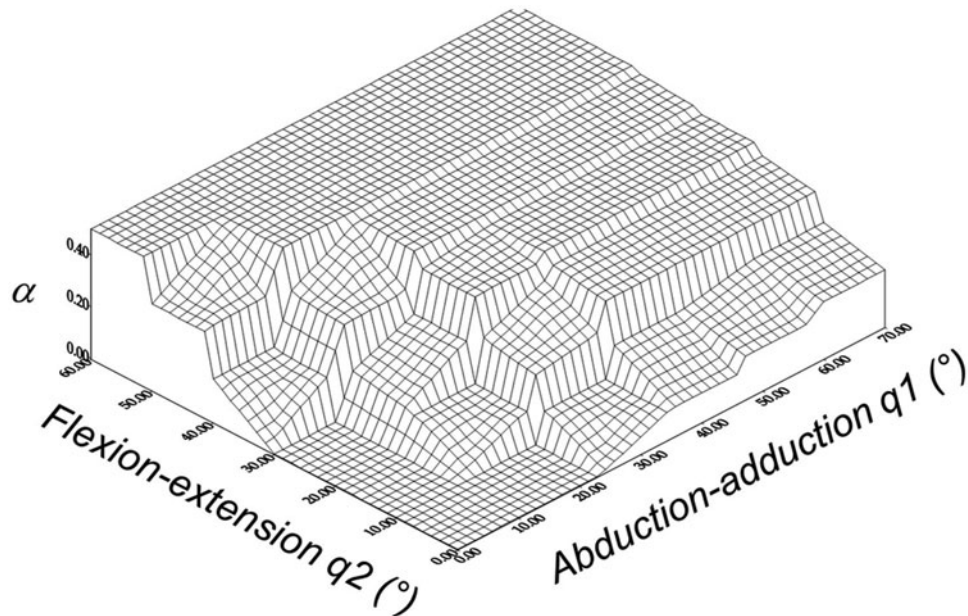
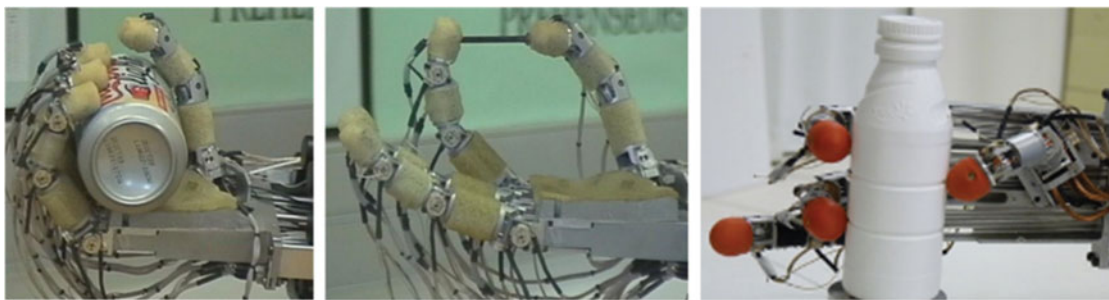Fig. 4. $\alpha = f(q1,q2)$ calculated with the fuzzy controller.

Fig. 5. Grasps with the LMS hand.

and to build, on demand, a specialized gripper for a given set of manipulation/inside hand/grasping tasks.

First of all, the success of a gripper/hand design depends on the development of an efficient finger design. Designing a good robotic device requires a high level mechatronics design methodology. This methodology has to create a synergy between the mechanical, electronic and control designs.

Based on this experience, the development focused on the following constraints for the mechatronics design:

- Each joint should be controlled independently, which implies the right finger kinematics choices that meet the manipulation requirements and also to ensure that the technology in the mechanical links maximizes the transparency of transmission.
- The backlash in the tendon-based transmission should be minimized by limiting friction.
- The joint torque calculation should integrate the rheological behavior of the tendons.
- The control should be simple and robust; this implies to use the same approach for controlling all fingers.

We chose to design a modular finger that we could assemble freely into hands. For the LMS hand, the thumb kinematics were similar to that of a human hand. With the new RoBioSS hand, the challenge of anthropomorphism in the design was not the priority, and our focus was on reproducing a human-level dexterity with a configuration of fingers on the palm similar to the human hand, with anthropomorphic dimensions.
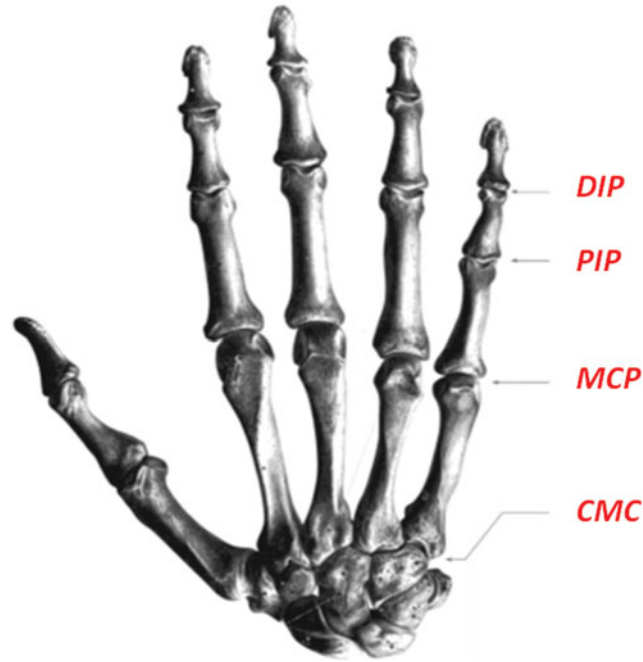
Fig. 6. Human hand skeleton.

Table I. Finger joint limits.

	$q1(°)$	$q2(°)$	$q3(°)$	$q4(°)$
Min (index, middle, ring)	−30	−90	−110	−110
Max (index, middle, ring)	30	90	110	110
Min (thumb)	−45	−90	−110	−110
Max (thumb)	90	90	110	110

As the choice of the finger's architecture is essential for dexterous performance, we have adopted the human finger anatomy shown in Fig. 6. Excluding the carpometacarpal joint (CMC), a human finger has four DoF: two DoF at the base of the finger for the MCP, one DoF for the proximal interphalangeal (PIP) joint, and the last DoF for the distal interphalangeal (DIP) joint.

The finger kinematic model is given in Fig. 7. Angle q_1 refers to the abduction–adduction movement of the finger while q_2, q_3, q_4 refer to the flexion–extension movements. O_0 is the base of the MCP joint and P is the fingertip. As we can observe on the model, the abduction–adduction and the flexion–extension axes of the MCP joint are not concurrent as it is the case in the human finger. The design of the joint will be explained in Section 2.2.

The choice of the finger dimensions given in Fig. 7 is explained in ref. [23]. The dimensions were fixed by using the human hand analysis. One of the advantages of remote actuation is that it does not limit the lengths between joints. Therefore, they can be optimized according to the task that the hand is built for. For instance, the dimensions of the phalanges could be easily adapted to the dimensions of the objects that the robotic hand would manipulate. The main objective of the robotic hand that we have built is to carry out tasks usually performed by humans; and/or collaborative tasks between human and machine; consequently the finger size should be close to an adult human finger as shown in Fig. 8.

Table I details the finger joint limits. These values demonstrate that the workspace is much wider than those of a human hand and also of the LMS hand. In order to have more human-like motions, we can restrict, with an appropriate software configuration, the joint limits to anthropomorphic values.

Based on this design, the weight of the finger structure made of aluminum alloy is 43 g and each actuator weighs 70 g. This adds up to a total weight of actuators equal to 1.12 kg and a hand weight of 1.8 kg with 16 actuators.
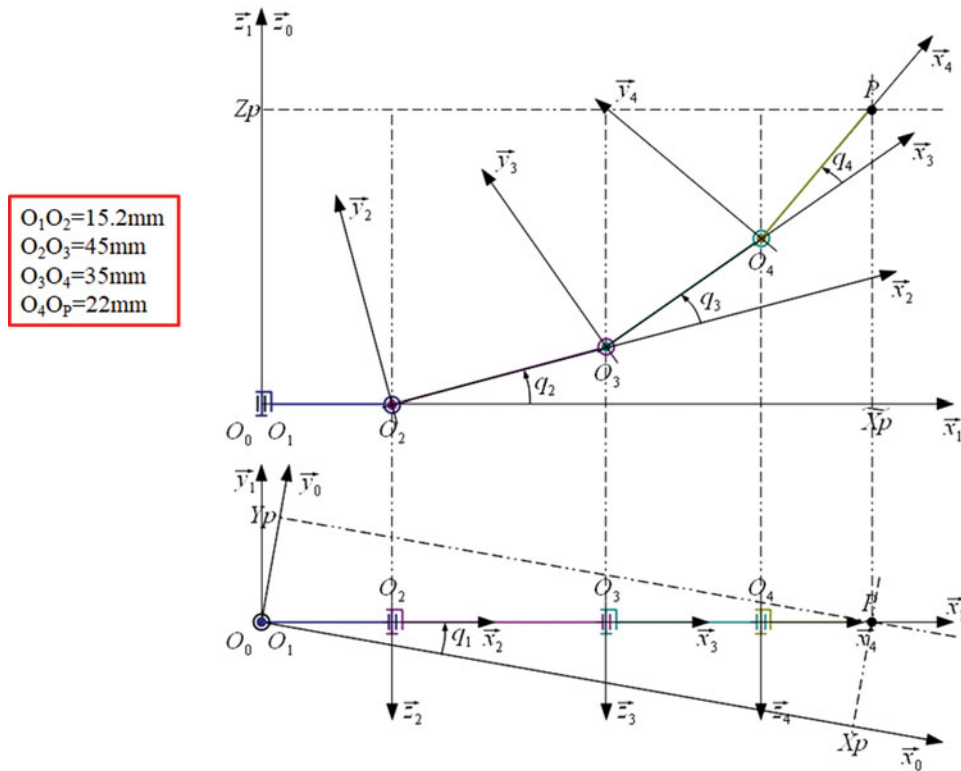
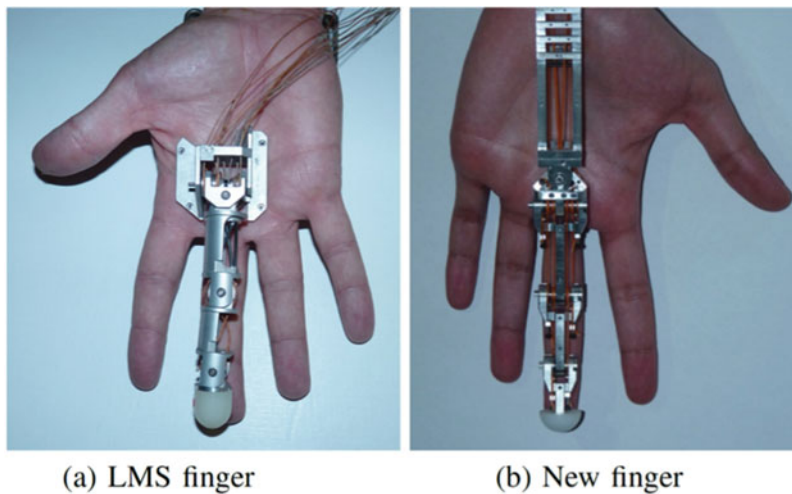Fig. 7. Finger kinematics and dimensions.

$O_1O_2 = 15.2\text{mm}$
$O_2O_3 = 45\text{mm}$
$O_3O_4 = 35\text{mm}$
$O_4O_P = 22\text{mm}$

(a) LMS finger   (b) New finger

Fig. 8. Size comparison with a human finger.

3. Tendon Actuation

3.1. Tendon routing
An efficient finger design first requires that the transmission between actuator motion and joint motion is clear with low static friction, low hysteresis, and that it features constant coupling relations between actuator and joint motions.

If these conditions are achieved, it becomes possible to coordinate all fingers in a real-time scheme for producing collaborative tasks between fingers. This process will be detailed in Section 4.

As we decided to base the design of the new hand as an assembly of finger modules, this leads to the same kinematics for all fingers and also to the same tendon routing technology. Nevertheless,
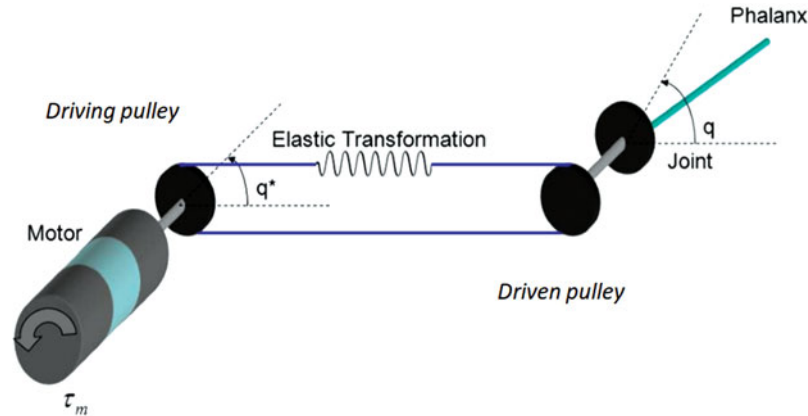
Fig. 9. Endless tendon routing.

fingers may be different because it is possible to choose different lengths for the finger phalanges. The segment lengths may be chosen by considering the tasks that the hand or gripper will have to achieve. As stated previously, for the new dexterous RoBioSS hand, the different lengths were inspired by human fingers.

The design choice of finger modules allows us to place the fingers on a palm or a frame base as required. It thus becomes possible to propose the design of a non-anthropomorphic gripper, useful in industrial applications for example. As the four finger joints are remotely actuated with four motors by using tendon-driven actuation, the design of the hand is not affected by the implementation of the actuation that could be remotely located in the forearm or next to the palm.

Another advantage of this actuation principle is the possibility of adapting the motors to the task without changing the finger design. For example, if a task requires higher torques, the motors could be easily replaced by more powerful ones and the interface adapted to the application.

For our new finger, we chose to use the endless type of tendon routing,[19] which enables the motor to drive the joint in both directions. The model of the transmission is given in Fig. 9. If the cable initial tension is too high, the joint friction makes the movement of the joint in both directions difficult. Therefore, a small screw-based mechanism allows to adjust the distance between axes, and thus the cable tension.

Figure 10 shows the tendon routing for the distal phalanx. In order to route the cables through the finger, intermediate pulleys are used. To ease the wiring of the finger, we use two cables instead of a single one to drive the pulleys, one for each direction of the joint. Here, the blue cable is for the flexion motion of the distal phalanx and the red one is for the extension motion. Each cable is attached to the driving pulley on one side, and to the driven joint on the other side as shown in Fig. 9.

The cable routing leads to the following joint coupling relation:

$$Q = A_f \cdot S$$

$$A_f = \begin{pmatrix} D_0/D_1 & 0 & 0 & 0 \\ 0 & D_0/D_1 & 0 & 0 \\ 0 & -D_2/D_1 & D_0/D_1 & 0 \\ 0 & (D_3 - D_2)/D_1 & -D_3/D_1 & D_0/D_1 \end{pmatrix}$$

where

$Q = [q_1 q_2 q_3 q_4]^T$ represents the finger joints values.

$S = [s_1 s_2 s_3 s_4]^T$ represents the actuator positions.

$D_0 = 10.2$ mm is the diameter of the driving pulley on the actuator axis and $D_1 = 10.2$ mm is the diameter of the driven pulley on the joint axis.

$D_2 = 8.6$ mm is the diameter of the intermediate pulley for the MCP joint. $D_3 = 7$ mm is the diameter of the intermediate pulley for PIP and DIP joints.
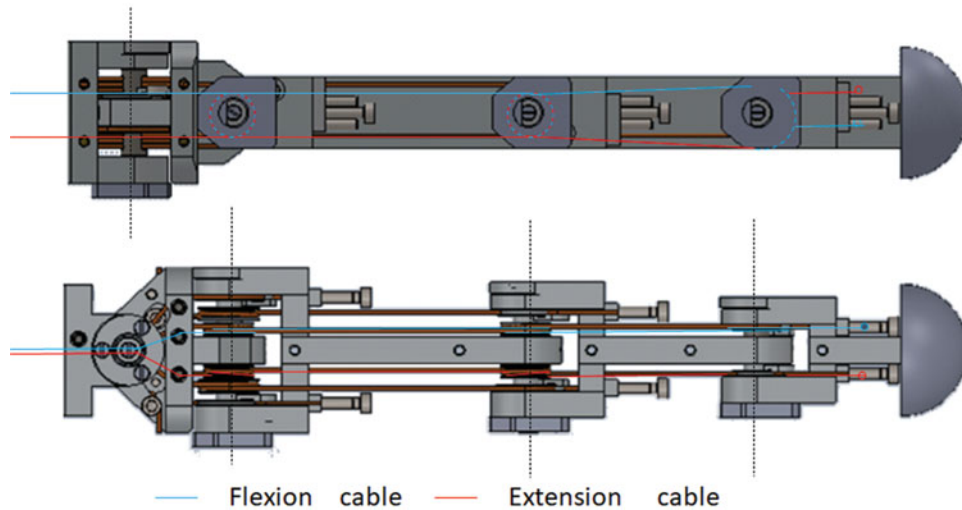
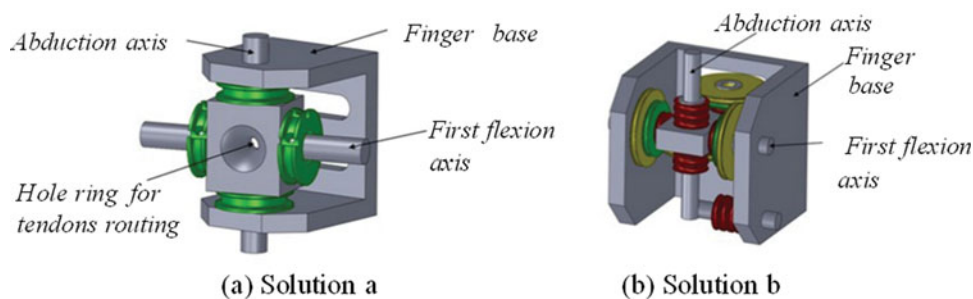Fig. 10. Cable routing for the distal phalanx.

Fig. 11. Universal joint designs.

3.2. MCP joint

One key element for the successful operation of the finger is the design of the MCP joint because the tendons for the PIP and DIP joints go through it. It is, therefore, important to route the cables through the joint in a way that avoids contact between them in order to reduce friction effects. We used the following design guidelines:

- Decoupling the flexion–extension joints from the abduction–adduction joint movement is a key element, which means the routing of each cable must ensure that cable length remains constant between actuator and joint during an abduction–adduction motion.
- Reduce friction acting along the tendon as much as possible by using pulleys and bearings.

Figure 11 shows two designs for a universal joint with concurrent axes respecting the guidelines. The main issue with solution (a) is that all the tendons have to go through the ring hole which increases friction between tendons significantly when there are more than two tendons going through it.

Solution (b) in Fig. 11 is an acceptable design and is used for example in the CEA dexterous hand[2] although it is not suitable for our finger because we needed to route six tendons, two per flexion, while maintaining the joint small enough to meet a human-size finger requirement. This solution is compatible with underactuation as is the case for the CEA dexterous hand. In this device, the fingers are not fully actuated: there is a coupling between the rotations of the distal phalanx and of the intermediate phalanx.

Consequently, to meet our design criteria, the solution was to have a MCP joint with non-concurrent axes. This change enables us to decouple the abduction–adduction motion and the flexion–extension motions of the finger. The selected design is shown in Fig. 12. As the cables go through the abduction–adduction axis, cable length remains theoretically constant between actuation and joint. From the
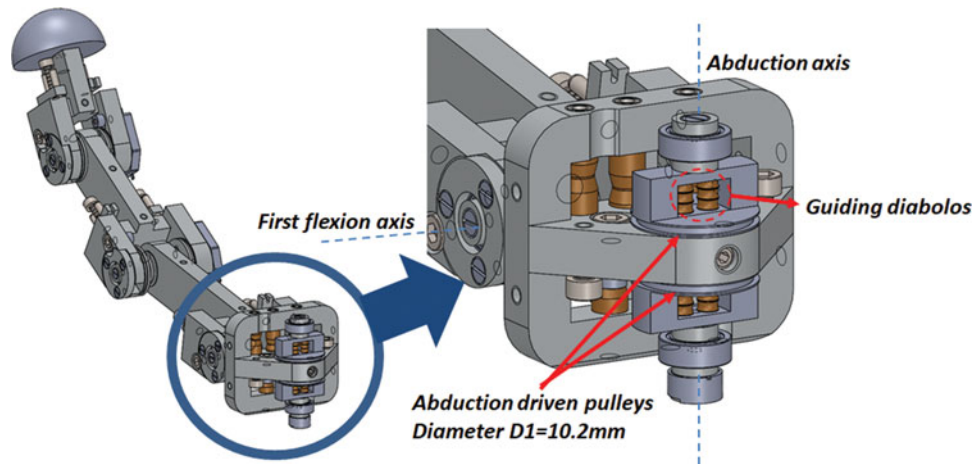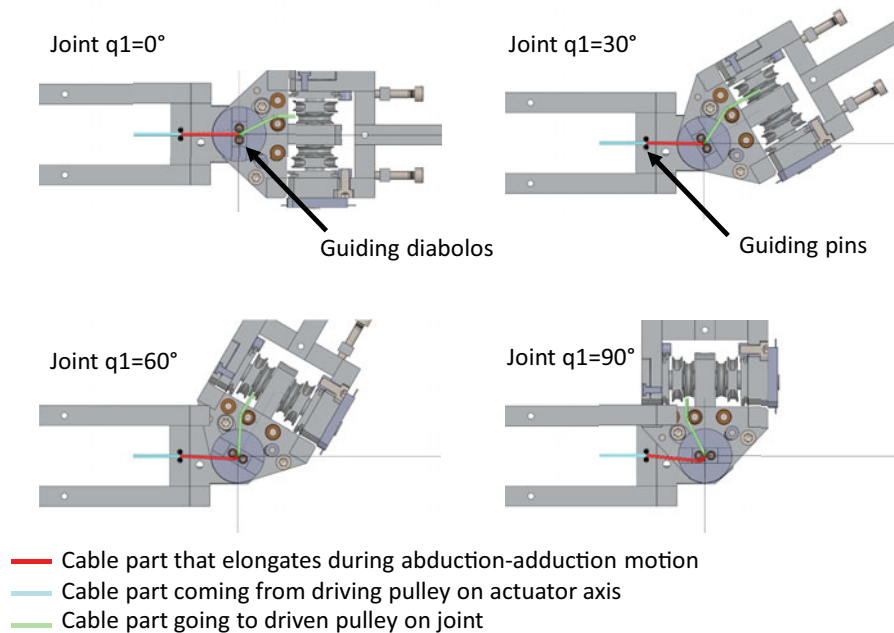
Fig. 12. MCP joint design.

Fig. 13. Sectional view of MCP joint tendon routing for proximal phalanx.

technological point of view, in order to limit friction and cable wear, we used guiding diabolo-shaped pulleys to ensure the routing of the tendon.

For each cable, two guiding diabolos (diameter 1.6 mm) are used to maintain the cable (diameter 0.6 mm) to go through the abduction–adduction axis. The winding of the cable on the pulley causes a very small elongation of the cable. This elongation is the same on the extension cable and on the flexion cable as described in Fig. 10. The result is a very small additional strain in the cable.

A sectional view of the MCP joint with its cable routing is shown in Fig. 13. Figure 13 illustrates the winding of the cable used for proximal phalanx movement. The principle remains the same for each actuated phalanx.

Figure 14 illustrates the small cable elongation at the MCP joint due to the use of guiding diabolos. Point A is located at the diabolo axis, point P at the center point of the two guiding pins (cf. Fig. 13); r is the winding radius on the pulley; L is the cable length between guiding pins and abduction–adduction axis; *Phi* corresponds to the winding angle on the diabolo and is linked with $q1$ joint value.
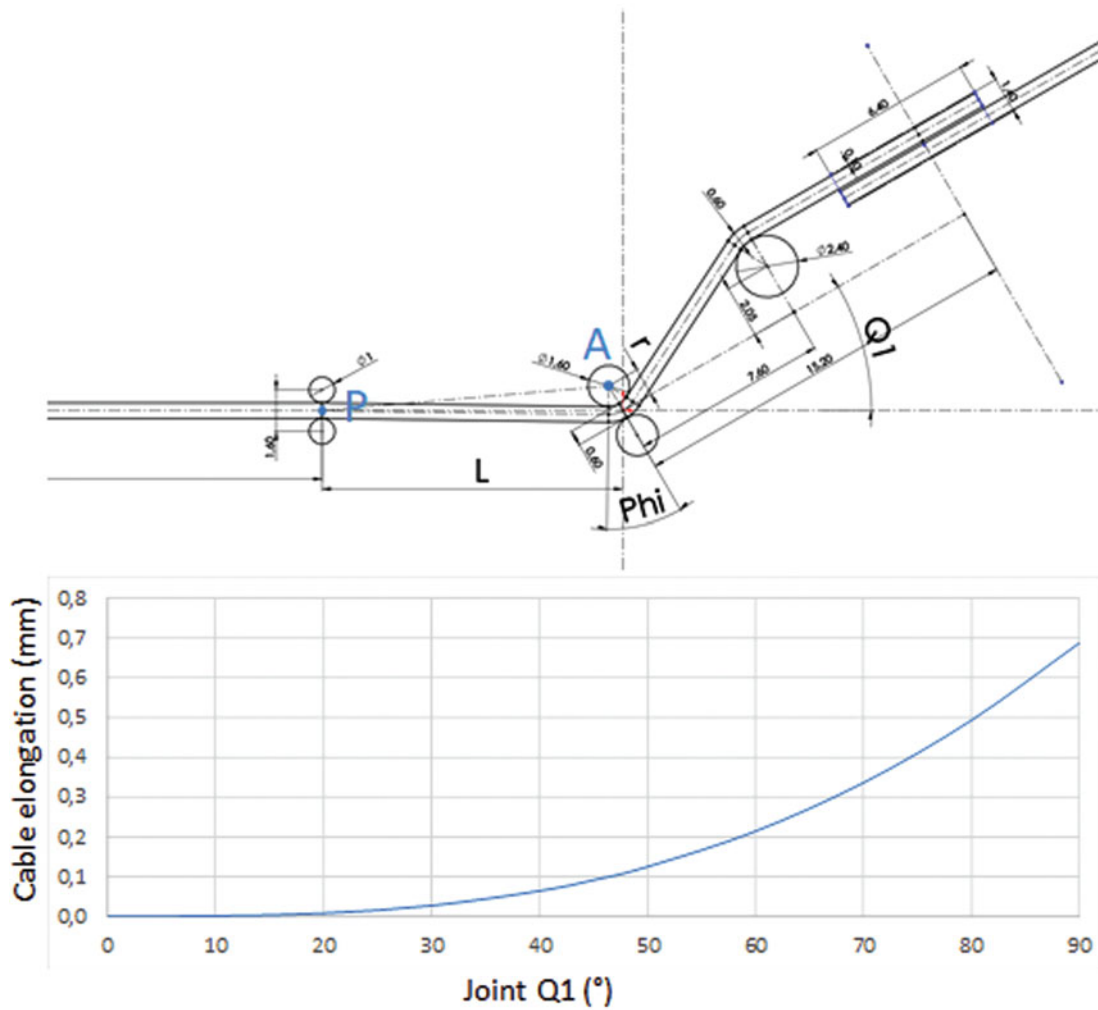
Fig. 14. Parameters for the evaluation of the cable elongation.

Thus, we can calculate the cable elongation based on these parameters definitions:

$$\left\|\overrightarrow{AP}\right\| = \sqrt{(L.\cos(Q1)^2 - (L.\sin(Q1) - r)^2}$$

$$Phi = \cos^{-1}\left(\frac{r^2 + \left\|\overrightarrow{AP}\right\|^2 - L^2}{2.r.\overline{\|AP\|}}\right) - \cos^{-1}\left(\frac{r}{\overline{\|AP\|}}\right)$$

$$\text{Cable elongation} = r.Phi + \sqrt{\left\|\overrightarrow{AP}\right\|^2 - r^2} - L$$

The computed elongation drawn in Fig. 14 illustrates the fact that the elongation is negligible if we consider an abduction–adduction motion (q1 joint) lower than $\pm30°$. This is the case for index, middle and ring fingers. For the thumb, the abduction–adduction motion may be greater, up to $90°$. The elongation remains small in this situation and corresponds to 0.2% cable elongation (cable length for the thumb is 350 mm).
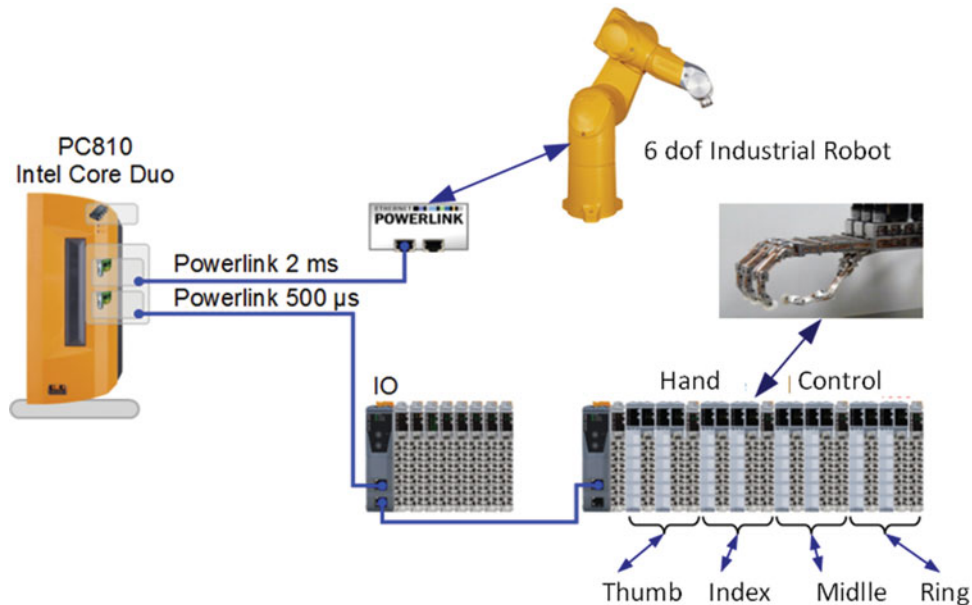
Fig. 15. The hardware control architecture of the new RoBioSS dexterous hand.

4. Experimental Validation

4.1. The control architecture for evaluating the hand

We developed the new RoBioSS dexterous hand to improve the patented finger design. The hand was designed to be used as an end-effector for an industrial robot or for a collaborative robot. The compactness of the proposed gripper is illustrated with the demonstration at SPS IPC Drives international exhibition.[27]

For experimental validation, the hand was mounted on a TX60 6-axis Stäubli serial robot (see Fig. 15) powered by a uniVAL drive industrial robotic controller, which offers the innovative feature of a possible integration with an external controller. All 22 axes are driven by a B&R Automation industrial PC (16 axes for the hand and 6 axes for the Stäubli robot). Communication between the robot controller, the DC motor power stages and the PC runs through a high speed real-time POWERLINK fieldbus, which guarantees that all motions are synchronized. Low level control loops for the hand motors also run on the industrial PLC. Robot-level software implements PLCopen Motion standard. In our application, all axes are given 2 ms periodic position commands.

In this section, the method used to evaluate the mechanical transparency of the transmission is based on the evaluation of the joint movements. For that purpose, the fingers produce free motions and have no load in order to have the same evaluation conditions used for the LMS hand in Section 1. The key point in this validation phase was to control only the actuators using motors encoders feedback S_act without taking into account a second loop with joint positions $Q_{potentiometer}$ feedback, as described in Fig. 16. The potentiometers are used for the evaluation of the joint motions and they will be used in the future for the evaluation of cable elongation. As there is no joint position feedback, we can estimate the joint precision control to $\pm 1°$ (cf. Fig. 18).

Figure 16 shows the control of the fingers; each finger uses four actuators. The finger control loop is implemented on an industrial PC (B&R PC810) with a cycle time fixed at 500 μs. A classical cascaded position–velocity–current loop with encoder feedback on the DC motor shaft is implemented. The control scheme also includes a prediction block at the input of the PI position loop, and a feed-forward block at the input of the current loop C_Set. An evaluation of dry friction (Coulomb coefficient) and viscous friction is also carried out for each actuator and included within the controller.

Before starting the motion, a joint trajectory is computed for each finger offline with our simulation software and manipulation planner.[26] This trajectory may concern a test trajectory, a grasping task using fingertips or an object motion inside the hand. As we control the motors, the motor commands are deduced from the joint positions by using the coupling matrix A_f presented in Section 3. An
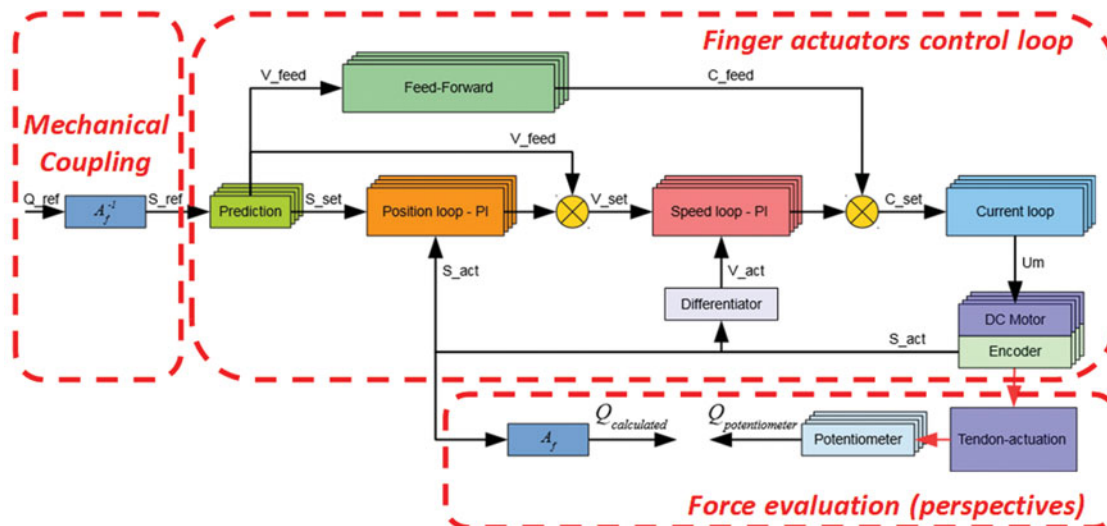
Fig. 16. Finger control loop for the four joints.

important evolution in the new finger is the fact that the coupling matrix uses constant values thanks to the improved mechanical design.

As illustrated in Fig. 16, the joint parameters Q_ref issued from the computed trajectory are sent to the controller every 2 ms by using the coupling relation:

$$S\_ref = A_f^{-1} \cdot Q\_ref$$

In the same period, the commands S_ref are sent to the actuator's control loop.

For the hand behavior evaluation, the theoretical joint position calculation is made by using the direct coupling relation with the motor encoder positions:

$$Q\text{calculated} = A_f \cdot S\_act$$

As the transmission is based on the use of an elastic cable (cf. Fig. 9), the difference between the joint theoretical position $Q_{\text{calculated}}$ and the measured joint position $Q_{\text{potentiometer}}$ provides the cable elongation. Within this experiment, the cable elongation is only due to the friction in the transmission. The joint torques will be evaluated by using a rheological model of the tendons, in a future study. This evaluation of joint torques based on tendon elongation is inspired by previous works.[1,21] For the LMS hand, a learning based method (neural networks) was used for the evaluation of the grasping forces. For our new hand, we intend to evaluate these forces directly from the cable elongations and the cable rheological law.

4.2. Analysis of unloaded fingers motions
For comparison purposes, we performed the same study as the one carried out on our first hand and presented in Section 1, Fig. 3. Figure 17 shows the potentiometers values of q3 and q4 while moving only q2 with different values of q1. These graphs validate the new MCP joint design discussed in Section 3 as we can observe that the coupling relation remains constant whatever the configuration of the abduction–adduction movement; it was not the case with the previous design of LMS hand (Fig. 3).

The transparency in the transmission of the new finger was evaluated with single axis motions in the previous study.[23] With these motions, the objective was to demonstrate that is was possible to independently control each joint. We would now like to improve the RoBioSS hand by demonstrating the synchronization of the motions of all axes of the hand. Figure 18 presents the results concerning this experiment, in which fingers produce a point to point motion involving all the actuators. This experiment concerns three fingers because stable inside hand manipulation task requires three fingers. The motion velocity is about 40°/s for each axis, acceleration is $400°/s^2$.
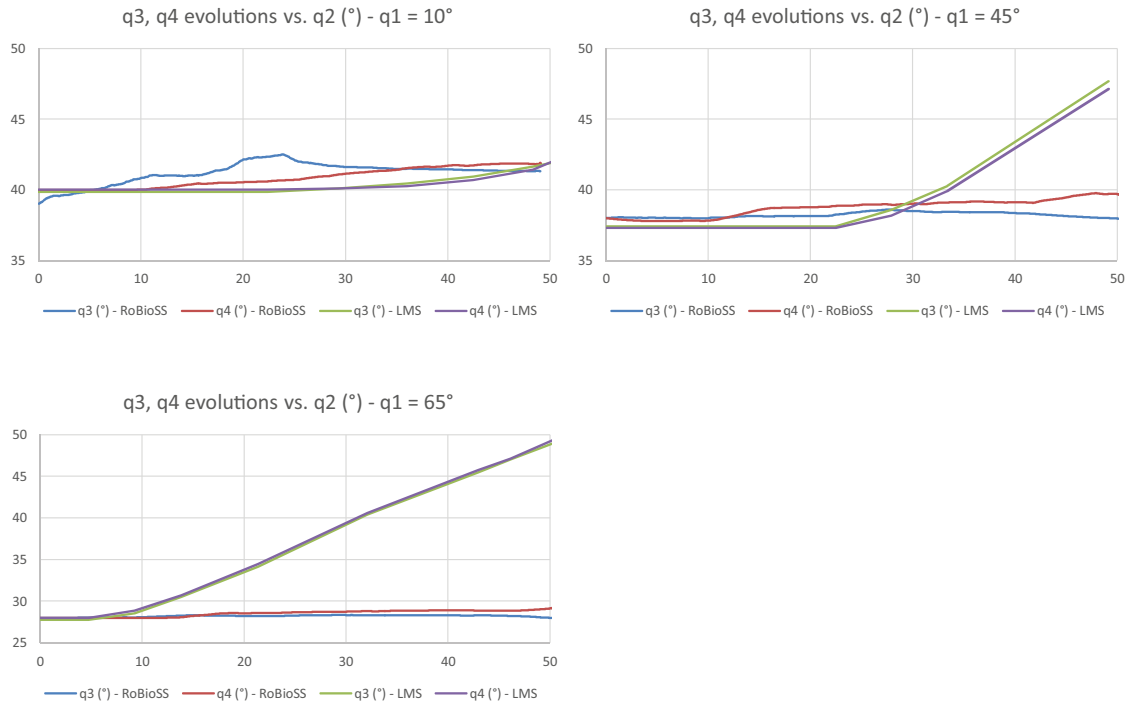
Fig. 17. Measures of q3 and q4 while moving q2 for different fixed values of q1.

The curves for all fingers illustrate a very small cable elongation for each actuated joint. The joint motion based on the encoder position feedback control provides a good synchronization of the fingers (each time phase is exactly the same) and a good tracking of the theoretical computed joint position using coupling relation. The difference between joint measure using potentiometer and computed joint value based on the use of the coupling matrix is less than $2°$.

The backlash is low, as all joints on all fingers start and stop their motions at the same time with a small latency between joints at the starting phase.

Figure 18 emphasizes the starting moments of the motions and illustrates this latency time for the joints of the middle finger. The velocity trapezoidal profiles for the four considered joints reveal a latency time of about 20 ms between the first starting joint and the last one. This time shift disappears during the acceleration phases.

In order to evaluate viscous friction in the transmission, we performed a dynamic motion (joint speed $70°$/s, acceleration $400°/s^2$) on each joint. Figure 20 presents the results for the MCP joint (Q4). It shows a small but constant difference between joint position (Q4_pot) and actuator position (Q4_ref) during each of the constant speed phases. This difference is about $2°$ and represents the viscous friction. Based on the cable stiffness $K = 0.007\%$/N, the corresponding viscous friction was evaluated and is about 0.04 Nm/rad/s; this low viscous friction can be easily integrated in the feedforward controller.

In order to evaluate viscous friction in the transmission, we performed a dynamic motion (joint speed $70°$/s, acceleration $400°/s^2$) on each joint. Figure 20 presents the results for the MCP joint. It shows a small constant difference between joint measure and actuator position during each of the constant speed phases. This difference is about $2°$ and represents the viscous friction. Based on the cable stiffness K = 0.007%/N, the corresponding viscous friction was evaluated and is about 0.04 Nm/rad/s; this low viscous friction can be easily integrated in the feedforward controller.

Figure 20 provides also information about dry friction as the difference goes back to $0°$ once the dynamic motion is achieved. This result is consistent with the one of Fig. 19 and also demonstrates that dry friction is negligible.

These experiments illustrate the behavior of the transmission and validate the hand design. As a conclusion, we can state that:
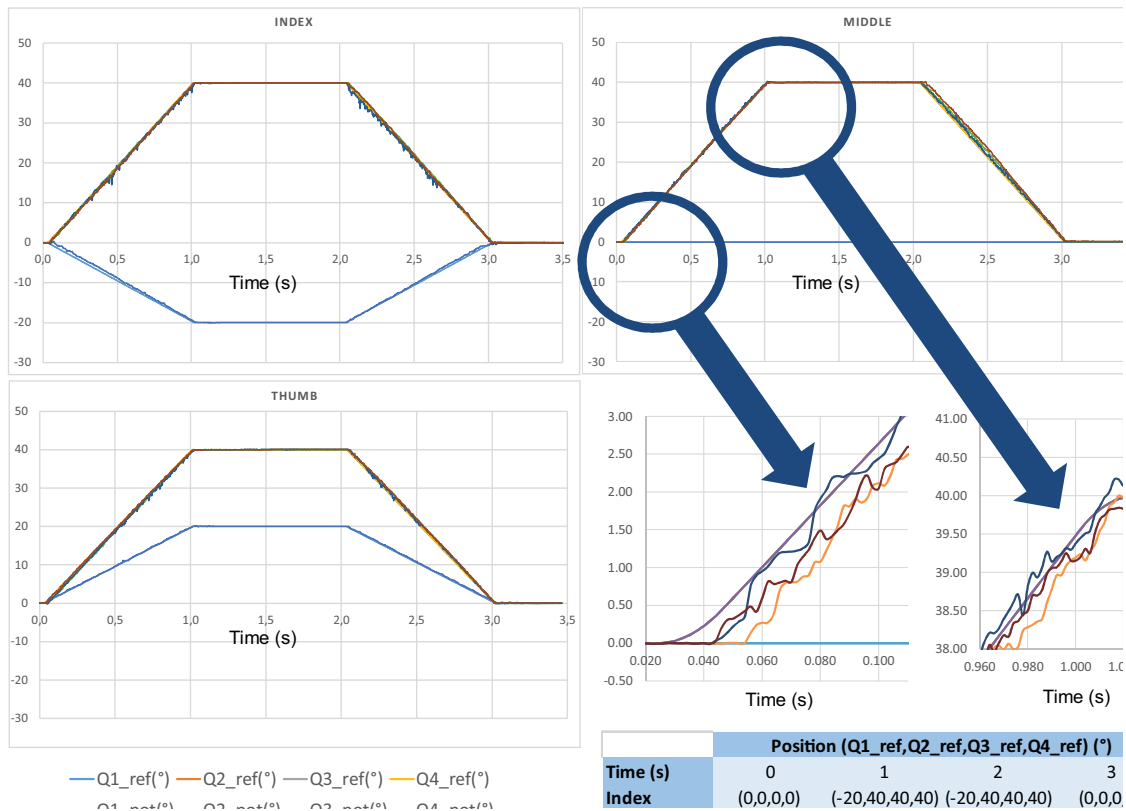
	Position (Q1_ref,Q2_ref,Q3_ref,Q4_ref) (°)			
Time (s)	0	1	2	3
Index	(0,0,0,0)	(-20,40,40,40)	(-20,40,40,40)	(0,0,0,

Fig. 18. Synchronized fingers motions, joint speed $40°/s$, acceleration $400°/s^2$.
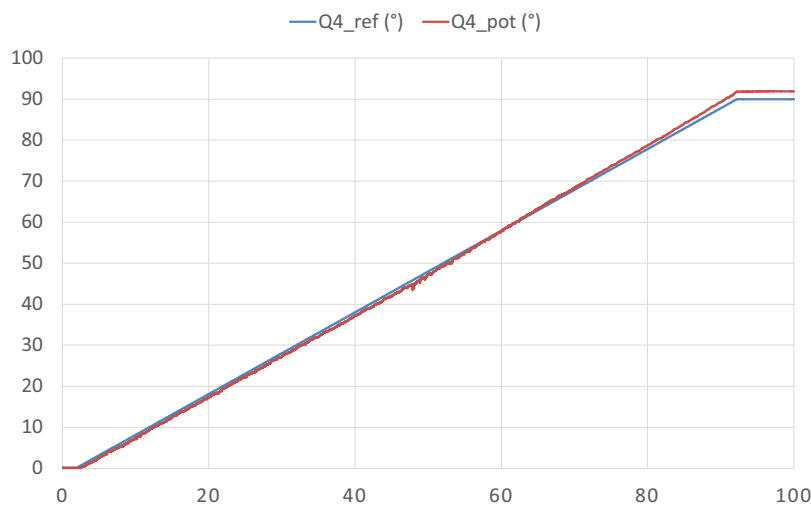

Fig. 19. Analysis of the dry friction (DIP joint).

- fingers phalanx inertia are negligible for manipulation purpose because of the low dynamics involved;
- static friction is negligible;
- viscous friction is low;
- the coupling matrix between joints and actuation is constant.

All these mechanical improvements led to the development of a hand design that facilitates the control without using complex control schemes. The average computation time for the 16 axes of the hand only based on encoder feedback is 40 μs.
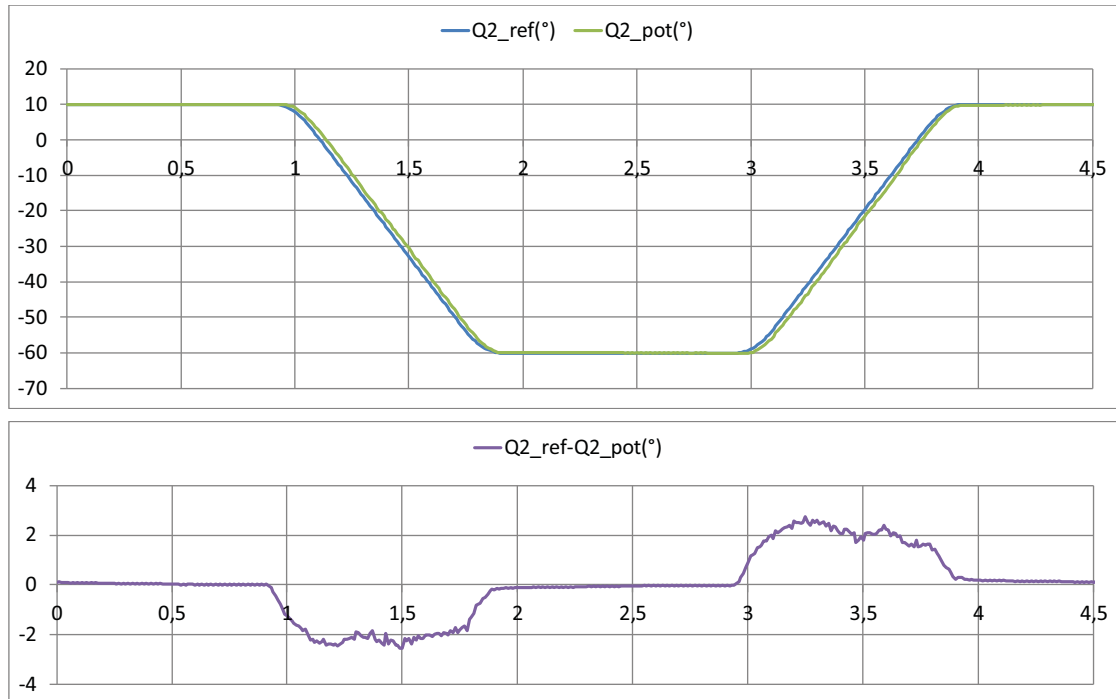
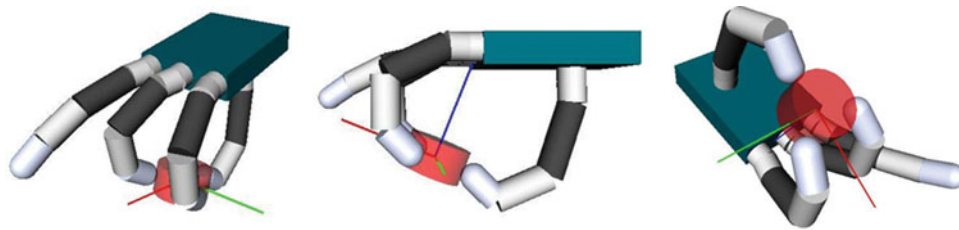Fig. 20. Analysis of viscous friction (MCP joint).

Fig. 21. Initial grasp synthesis for the screwing of the bottle cap.

The implementation of a joint torque estimator based on the rheological model of the cable will be simpler than the one for our previous hand. The difference between $Q_{\text{calculated}}$ and $Q_{\text{potentiometer}}$ for contact force evaluation was discussed in ref. [21]. However, with this new design, we will be able to access the fingertip contact force without having to use neural networks. The results will be detailed in future work.

4.3. First results with an inside hand manipulation task

The objective of the first manipulation task that we carried out was to evaluate the inside hand manipulation capability. In particular, we wanted to know how the three fingers were able to collaborate for screwing and unscrewing a bottle cap. Two types of object motions are shown in this example: the rotation of the cap and the translation of the cap. The Stäubli robot is only used during the reach motion for the placement of the hand next to the bottle.

We used our motion planning strategy and software[26] to generate the joint trajectories for the screwing of the bottle cap. The initial grasp is illustrated in Fig. 21. Initial grasp synthesis is described in a previous work.[27]

The video[28] shows a good synchronization between the three fingers involved in this inside hand manipulation task. The hand will be improved in the near future for collaborative tasks with humans.

Figure 22 illustrates some of the steps of the experiment. One can observe on video[28] the translation motion for extracting the cap. This translation motion illustrates the good synchronization of the three fingers motions and the passive compliance of the fingers that contributes to balance the grasp.
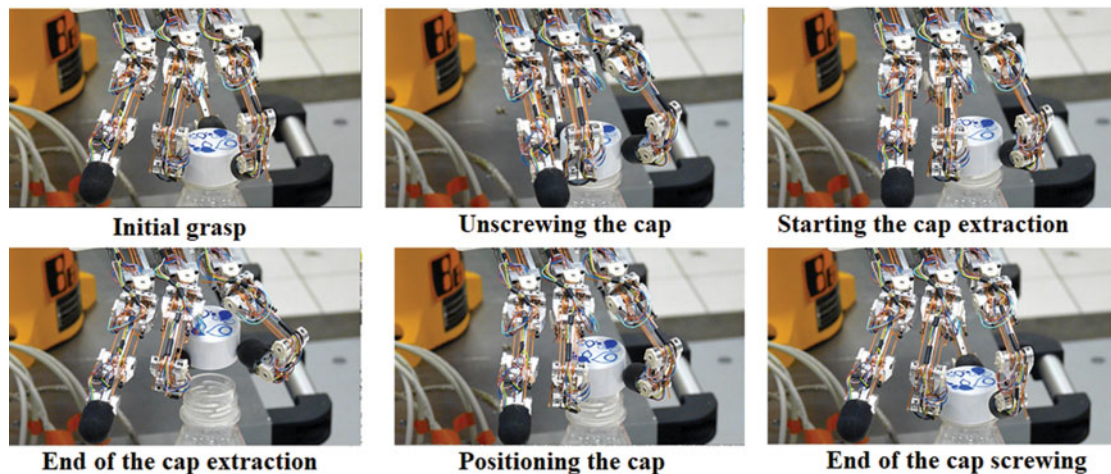
| Initial grasp | Unscrewing the cap | Starting the cap extraction |
| End of the cap extraction | Positioning the cap | End of the cap screwing |

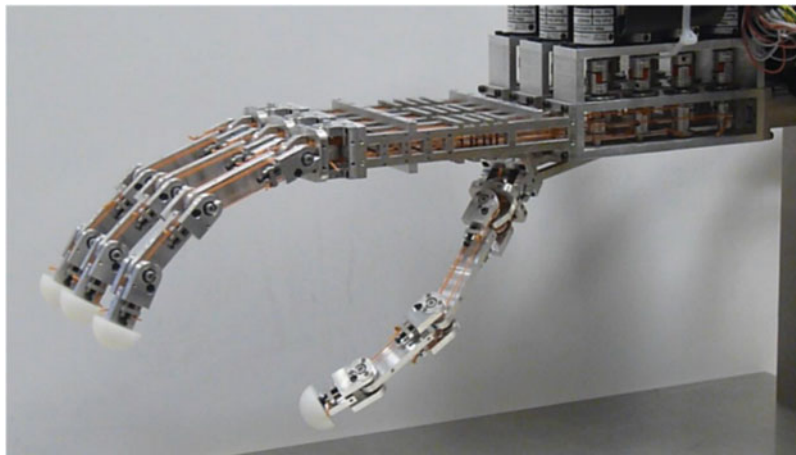Fig. 22. Unscrewing, extracting and screwing the bottle cap.

Fig. 23. The new ROBIOSS hand.

5. Conclusion

In this study, we have proposed a mechatronics design for a new dexterous robotic hand. The fingers are bio-inspired by human hand kinematics; each finger has four actuated DoFs, one for the abduction–adduction movement and three for the flexion–extension movements. One of the main challenges was to be able to build a mechanism with an average adult finger size. Most of the existing fully actuated dexterous robot hands designed for inside hand manipulation are not human-sized: it is very difficult to succeed on such a small scale with real in-hand manipulation capabilities.

This paper focused on the design guidelines that we established thanks to many years of development in the field of dexterous grippers. The tendon routing and MCP joint design has been extensively detailed. The main focus for the design was to reduce friction by using pulleys and bearings, to avoid mechanical non-linearities and reduce cable wear. An innovative MCP joint design was presented: it completely decouples the abduction–adduction movement and the flexion movements in order to improve controllability.

The transmission and the finger behavior were tested and evaluated. The different experiments demonstrate that the design goals were reached. A patent application has been submitted for this new finger design.[22]

We used this finger module to build the anthropomorphic hand shown in Fig. 23. In our future work, we will model the cable flexibility to estimate the finger contact force and evaluate the accuracy of this method. We will also assess the hand's capacity for in-hand manipulation by implementing the algorithms presented in ref. [26]. As a demonstration of the hand achievements, two videos are

available on the links.[27,28] They both show the synchronization of the fingers which produce fine object motions inside hand: fine rotations around any direction, and fine translations. The grasp stability is ensured and the robot robustness was validated in Nuremberg during the international exhibit.[27]

Our hand design is a sound core principle for building efficient hands or gripping devices for collaborative robotics and also human–machine interaction. A search within the international robotics research community reveals that there are a few hands able to produce fine motions of the grasped object inside hand; such a development requires a collaboration scheme between the fingers. Each finger behaves like a robot; and a three finger inside hand manipulation requires the ability to control each finger/robot within a real-time hybrid force/position cooperative control scheme. The RoBioSS hand has proven its ability to provide such a behavior with our first results and video demonstrations.

References

1. J. P. Gazeau, S. Zeghloul and G. Ramirez, "Manipulation with a polyarticulated mechanical hand: A new efficient real-time method for computing fingertip forces for a global manipulation strategy," *Robotica* **23**, 479–490 (2005).
2. J. Martin and M. Grossard, "Design of a fully modular and backdrivable dexterous hand," *Int. J. Robot. Res.* **33**(5), 783–798 (Feb. 2014).
3. S. R. Company, "Design of a Dextrous Hand for advanced CLAWAR applications," *Proceedings of the International Conference on Climbing and Walking Robots and the Supporting Technologies for Mobile Machines, no. C* (2003), pp. 691–698.
4. M. Grebenstein, M. Chalon, W. Friedl, S. Haddadin, T. Wimböck, G. Hirzinger and R. Siegwart, "The hand of the DLR hand arm system: Designed for interaction," *Int. J. Robot. Res.* **31**, 1531–1555 (2012).
5. G. Palli, C. Melchiorri, G. Vassura, U. Scarcia, L. Moriello, G. Berselli, A. Cavallo, G. De Maria, C. Natale, S. Pirozzi, C. May, F. Ficuciello and B. Siciliano, "The DEXMART hand: Mechatronic design and experimental evaluation of synergy-based control for human-like grasping," *Int. J. Robot. Res.* **33**(5), 799–824 (Apr. 2014).
6. J. Falco, *A Roadmap to Progress Measurement Science* in *Robot Dexterity and Manipulation* (National Institute and of Standards Technology, US Department of Commerce, 2014) http://dx.doi.org/10.6028/NIST.IR.7993.
7. C. Melchiorri and M. Kaneko, "Robot hands," **In**: *Springer Handbook of Robotics* (B. Siciliano and O. Khatib, eds.) (Springer International, 2008). https://www.springer.com/us/book/9783540303015
8. K.-C. Nguyen and V. Perdereau, "Fingertip Force Control for Grasping and In-Hand Manipulation," HANDLE Training Workshop for Young Researchers and Ph.D. students, Benicassim, Spain (Feb. 2012).
9. V. Kumar, Z. Xu and E. Todorov, "Fast, Strong and Compliant Pneumatic Actuation for Dexterous Tendon-Driven Hands," *Proceedings of IEEE International Conference on Robotics and Automation* (2013).
10. C. Lovchik and M. Diftler, "The Robonaut Hand: A Dexterous Robot Hand for Space," *Proceedings of IEEE International Conference on Robotics and Automation* (1999).
11. M. Grossard, J. Martin and G. Felippe, "Control-oriented design and robust decentralized control of the CEA dexterous robot hand," *IEEE/ASME Trans. Mechatron.* **20**(4), 2015.
12. L. Cui, J. Sun and J. Dai, "In-hand forward and inverse kinematics with rolling contact," *Robotica* **35**(12), 2381–2399 (2017). doi:10.1017/S026357471700008X.
13. Akio Namiki, Yoshiro Imai, Masatoshi Ishikawa and Makoto Kaneko, "Development of a High-speed Multifingered Hand System and Its Application to Catching," *Proceedings of the 2003 IEEE/RSJ International Conference on Intelligent Robots and Systems*, Las Vegas (Oct. 30, 2003) pp. 2666–2671.
14. V. Bundhoo and E. Park, Design of An Artificial Muscle Actuated Finger Towards Biomimetic Prosthetic Hands," *Proceedings of the 12th International Conference on Advanced Robotics, 2005* (2005) pp. 368–375.
15. M. C. Carrozza, G. Cappiello, S. Micera, B. B. Edin, L. Beccai, and C. Cipriani, "Design of a cybernetic hand for perception and action," *Biol. Cybern.* **95**, 629–644 (2006).
16. Y. Kurita, Y. Ono, A. Ikeda and T. Ogasawara, "Human-sized anthropomorphic robot hand with detachable mechanism at the wrist," *Mech. Mach. Theory* **46**, 53–66 (2011).
17. Z. Xu, V. Kumar and E. Todorov, "A low-cost and modular, 20-DOF anthropomorphic robotic hand: Design, actuation and modeling," *13th IEEE-RAS International Conference on Humanoid Robots* (2013) pp. 368–375.

18. L. Birglen, T. Laliberté and C. Gosselin, Underactuated Robotic Hands(Springer Tracts in Advanced Robotics), vol. **40** (Springer International, 2008). https://www.springer.com/la/book/9783540774587
19. L. Odhner and A. Dollar, "Dexterous Manipulation with Underactuated Elastic Hands," *Proceedings of the IEEE International Conference on Robotics and Automation*, Shanghai (May 9–13, 2011) pp. 5254–5260.
20. M. C. Carrozza, C. Suppo, F. Sebastiani, B. Massa, F. Vecchi, R. Lazzarini, M. R. Cutkosky, and P. Dario, "The spring hand: Development of a self-adaptive prosthesis for restoring natural grasping," *Autonomous Robots* **16**, 125–141 (2004).
21. J. P. Gazeau, S. Zeghloul, M. Arsicault and J. P. Lallemand, "The LMS Hand: Force and Position Controls in the Aim of the Fine Manipulation of Objects," *Proceedings of the IEEE International Conference on Robotics and Automation* (2001), pp. 2642–2648, vol. **3**.
22. CNRS, "Doigt robotique modulaire pour la prehension et la manipulation dextre," Patent FR 1459956, 10 16, 2014.
23. H. Mnyusiwalla, P. Vulliez, J. P. Gazeau and S. Zeghloul, "A new dexterous hand based on bio-inspired finger design for inside-hand manipulation," *IEEE Trans. Syst., Man, Cybern.: Syst.* **46**(6), 809–817 (2016).
24. L. Biagiotti, F. Lotti, C. Melchiorri and G. Vassura, *How Far Is the Human Hand? A Review on Anthropomorphic Robotic End-effectors*, (DIES Internal Rep., Tech. Rep., Univ. Bologna, Italy, 2004).
25. Y.-H. Lee and J.-J. Lee, "Modeling of the dynamics of tendon-driven robotic mechanisms with flexible tendons," *Mech. Mach. Theory* **38**(12), 1431–1447 (Dec. 2003).
26. N. Daoud, J. Gazeau, S. Zeghloul and M. Arsicault, "A real-time strategy for dexterous manipulation: Fingertips motion planning, force sensing and grasp stability," *Robot. Auton. Syst.* **60**(3), 377–386 (Mar. 2012).
27. The RoBioSS hand in Nuremberg SPS-IPC International Exhibit: https://www.youtube.com/watch?v= X87KKuVESS8
28. The RoBioSS hand video cited in the newspaper "Le Monde" (Keywords: Le Monde – Gazeau) follow the link: https://www.youtube.com/watch?v=O_P69haNA4A